1967

A determination of dewetting in a biaxial stress field.

Juliano, Julius Robert

Monterey, California. U.S. Naval Postgraduate School

A DETERMINATION OF DE-WETTING IN A BIAXIAL STRESS FIELD

JULIUS ROBERT JULIANO

A DETERMINATION OF DEWETTING IN A BIAXIAL STRESS FIELD

by

Julius Robert Juliano
Lieutenant Commander, United States Navy
B.S., Naval Academy, 1958

[redacted]

Submitted in partial fulfillment of the
requirements for the degree of

MASTER OF SCIENCE IN AERONAUTICAL ENGINEERING

from the

NAVAL POSTGRADUATE SCHOOL

June 1967

ABSTRACT

An experimental investigation of dewetting in uniaxial and biaxial stress fields was conducted for infinitesimal strain levels. An optical technique was attempted with limited success, which demonstrated the need for more precise measurements at small strains. A method was developed for stiffening the surface of the propellant test specimen with commercial bonding cement, which facilitated the use of strain gages on the stiffened surface. An analytic expression was derived which relates measurements made on the outer surface of the cement to internal propellant behavior.

It was noted that dewetting commenced at strain levels of the order of zero strain, and that there was little variation with stress ratio in the strain at which dewetting commenced. Dewetting appeared to be complete at lower strains for higher stress ratios.

Dewetting was noted to be at such low strain values that the phenomenon is considered to be inconsequential in a practical engineering analysis of this propellant.

ERRATA SHEET

1. Page 2, par 3, line 2 and 3 should read engineering vice engineering.

2. Page 10, par 2, last line should read data vice date.

3. Page 31, last line should read [10] vice 10.

4. Page 39, item 10 should read dilatation vice dilitation.

TABLE OF CONTENTS

LIST OF TABLES

LIST OF ILLUSTRATIONS

TABLE OF SYMBOLS

E	Modulus of Elasticity of propellant (psi)
E_c	Modulus of Elasticity of cement or case (psi)
L	Length (in)
P	Load (lbs)
R	Stress Ratio
W	Half Width of propellant (in)
a	Radius of center bore in cylindrical propellant (in)
b	Radius of outer surface of propellant grain, or half thickness of propellant specimen (in)
h	Thickness of cylindrical case or of cement coat (in)
p'	Interface pressure (psi)
t	Half thickness of propellant (in)
t_c	Thickness of cement (in)
u	Displacement in the X direction (in)
v	Displacement in the Y direction (in)
w	Displacement in the Z direction (in)
α	A dimensionless constant
β	A dimensionless constant
ε_i	Strain in the i direction (in/in)
σ_i	Stress in the i direction (psi)
ν	Poisson's Ratio
ν'	Apparent Poisson's Ratio

ACKNOWLEDGMENTS

The author gratefully acknowledges the guidance, patience, understanding, and professional example rendered by Professor Gerald Lindsey during the completion of this project.

The author also gratefully acknowledges the assistance of United Technology Center, which supplied the propellant for the tests and the strain-dilatometer date of the propellant.

CHAPTER I

INTRODUCTION

Solid propellants are normally composite materials consisting of particles of a metallic compound (a filler) uniformly embedded in a matrix of elastomeric material (a binder). When the propellant is subjected to strain, the adhesive bond between filler particles and binder is likewise strained. If this bond is broken, the material is said to dewet. This dewetting process causes vacuoles to form, which in turn leads to an increase in volume. This phenomenon not only affects the chemical properties such as burning rate and susceptibility to detonate, but also certain physical properties such as the Elastic Modulus and Poisson's Ratio. It is therefore advantageous to be able to predict the dewetting point and dewetting characteristics of a propellant.

Thor L. Smith [2] studied the mechanical properties of composites consisting of small diameter glass beads embedded in a polyvinyl rubber compound. Elongated ringlike specimens were extended in a liquid dilatometer and the volume increase was measured as a function of extension. He found that at small strains the volume remained constant and above a critical strain, or Yield Point, the volume increased because of the formation of vacuoles around the beads. Above the Yield Point, Poisson's Ratio was calculated from the rate of volume change with extension and was found to be independent of strain and temperature.

A search began for a reliable method of measuring the volume change and the accompanying change in Poisson's Ratio, since these changes are direct indications of dewetting. This search led to the design of a number of different devices. One of the more successful devices is the dilatometer.

A dilatometer is essentially a chamber of constant volume in which a test specimen is placed and enclosed in either a gas or liquid. When the test specimen is strained to the point where its volume increases, the pressure in the gas increases due to its decrease in volume. In a liquid dilatometer an amount of liquid equal to the change in volume of the specimen is allowed to escape from the chamber. The change in pressure of the gas, or the amount of liquid displaced is measured and related to volume change.

Stedry, Landel, and Shelton [3] used a circular ring specimen in such a device, but they referred to it as a hydrostatic weighing device. Their results appeared to be reproduceable. They found, however, in contrast to Smith's [2] work on glass beads, that Poisson's Ratio for an actual propellant varied with strain from the onset of straining.

Rainbird and Vernon [5] at the Explosives Research and Development Establishment conducted a considerable amount of research with various devices. They devised a rheohydrometer, which was essentially a liquid dilatometer with provisions for carrying out tension and compression tests. These tests in the rheohydrometer produced

results similar to those of Stedry, et al, at the Jet Propulsion Laboratory, but dewetting started as low as zero strain in some cases, and not until 20% strain in others (dependent on temperature, propellant, and humidity).

Bells, Hart, and Holland [8] used a liquid dilatometer which was designed to provide volume change measurements while a specimen was being uniaxially strained at a constant rate. They used their experimental observations to derive a relation between the axial strain and the volume change. The relation involved one material constant, which was found to be the derivative of the first strain invariant with respect to the second strain invariant. This constant was found to vary with test temperature and filler content.

Farris [10] developed a model which describes the stress-strain and dilatation-strain relationships of solid propellants in terms of their frequency of dewetting. This model enables one to calculate the frequency of dewetting versus strain from the strain-dilatation relationship. Farris [11] also related the mechanical response and failure of these propellants to the formation and growth of vacuoles, which cause strain dilatation in the material. He used a statistical interpretation of the strain-dilatation behavior to assess both the instantaneous frequency of vacuole formation and the total accumulation. This provided an analytical method of describing the initiation and extent of microscopic failures within the material for uniaxial tension. Farris' strain-dilatation data were obtained with the use of a gas dilatometer.

The Thiokol Chemical Corporation [12] developed a method of obtaining volumetric responses of solid propellants utilizing an optical device developed by their Elkton Division. This device enabled the experimenter to obtain data without direct contact with the specimen and is adaptable to most standard tensile testers (e.g., Instron). The device consists basically of measuring the change in distance between the edges of the test specimen. This is accomplished by projecting a light on the specimen, then measuring the dark space on a mirror on the opposite side of the specimen from the light. Lenses are used for high resolution and photoelectric cells for high speed timing. In this research the experimenter found that dewetting may begin at strains as high as 21% and the point at which dewetting begins varies inversely with strain rate and hardness of the material. At low temperatures and low strain, the dewetting point is generally masked by this experimental method.

Microtensile test specimens have also been used. Rastrelli and Dehart [7] developed a method of measuring strain within solid propellants involving the electronic observation of embedded particles. This is relating the dewetting process to a microscopic level. The method consisted of the utilization of two basic systems. First, the scintillation facility, consisting of an x-ray passing through the specimen to a crystal detector. The detector output was converted to a relative count rate. The second system was the specimen loading device, which was constructed to allow the loaded specimen to index vertically, horizontally, or rotationally with reference to fixed x-ray

beam position. Specimens of varied shape, size, casting techniques, grain size, and embedded particle size were tested under loads producing up to 20% strain. They concluded that the initial strain distribution may not be uniform or simply related to external strain. They believed that their technique was particularly useful when applied to opaque solid propellant grains, in that it would be possible to precisely and clearly define the internal as well as the surface strain in a propellant.

Rainbird and Vernon [5] also used micro-tensile tests developed at A.B.L. and at Aerojet General, Azusa. The strips of propellant used in these tests were 0.005 in. thick, and their action under strain was observed. It was noted that in using this method dewetting occurred around the larger pieces of filler first. In some tests, dewetting did not occur before the specimen fractured.

A number of biaxial tests were also developed (although not always for the purpose of studying dewetting), and considered as candidates for this study. For example, Rainbird and Vernon [9] studied the behavior of propellants under multiaxial stresses. They devised a biaxial test in which a thin diaphragm of propellant was subjected to a pressure on one side. Varying stress ratios were obtained by using elliptical membranes of different axis ratios. In their tests with the membrane the major finding was that while dewetting spreads in bands under uniaxial loading, it is sudden and complete in this biaxial specimen. This was attributed to the pressure being maintained so that

the sudden reduction in Modulus at dewetting results in a sudden expansion of the diaphragm and complete dewetting.

Spangler [6] , working at the Eastern Laboratory of the duPont de Nemour Company, devised a test consisting of blowing a bubble of a thin disc of propellant supported at the edges. This technique was essentially the same as that used by E.R.D.E. [5] . Stress measurements were obtained analytically from relating: pressure measurements inside, radius of curvature, and thickness of the bubble. Strain values were obtained by photographic means or by the extensometer mounted on the bubble.

The complexity of these tests, and the indefinite results, led to the selection of a test specimen which was simple and could be handled with a minimum of complex equipment. The specimen was the same type as used by E.R.D.E. [5] .

A search of the literature available indicates that the phenomenon of dewetting of a uniaxially loaded solid propellant is well defined and is primarily dependent upon the maximum principal strain in the propellant. The characteristics of the propellant before, during, and after dewetting can be determined using one of a number of experimental techniques.

The effects of dewetting on the fracture properties of a solid propellant under biaxial loading have also been investigated and are fairly well defined. However, other characteristics such as Modulus and Poisson's Ratio are not well defined in this stress field. The

dewetting range and the criterion of dewetting have not yet been described as a function of biaxial stress ratio, for example.

The purpose of this thesis was to attempt to:

1. Measure initiation of dewetting in a typical ammonium perchlorate filled solid propellant under biaxial stress fields.

2. Establish a dewetting criterion suitable for both uniaxial and biaxial stress fields.

3. Generalize the criterion to arbitrary stress or strain states.

CHAPTER II

UNIAXIAL DEWETTING

As noted previously, most of the researchers in the field used either gas or liquid dilatometry. These devices produce good results for uniaxial tests, but they become almost prohibitively complex for the biaxial case. Additionally, one intuitively feels that there may be inherent errors in this method caused by an inability to separate the volumetric response of the propellant undergoing strain and by pressure-sensing fluid seeping into the vacuoles formed on the surface during the dewetting process.

Diaphragms, microtensile tests, and diffraction techniques were considered far too complex in the biaxial area to be utilized at the strain level at which the experiment was to be conducted. Furthermore, it is desirable to conduct a test and obtain measurements without any of the measuring devices coming in direct contact with the material, since almost all of the devices in use for metals (strain gages, variable reluctance gages, etc.) will effectively stiffen a low modulus material to the point where its properties are substantially changed.

Optical Measurements

It was decided to obtain Poisson's Ratio (ν) and the Elastic Modulus (E) by optical means. The method consisted of forming a standard tab end specimen, applying a load to it, and measuring the

changes in length with a high power microscopic comparator. It was hoped that a change in the slope of the stress-strain curve would be the indication of dewetting and that the use of the comparator would have as a by-product the ability to visually verify dewetting through the formation of vacuoles on the surface of the propellant. The comparator used was produced by the Gaetner Scientific Co., and reportedly had the capability of measuring to within 0.0005 inches with good accuracy. Small load increments, on the order of 0.1 to 0.2 lbs, were applied to specimens with different loading rates.

Ten tests were performed with loading rates varying from 0.10 to 0.50 psi/min with time intervals between loads of 5 or 10 min. It was found that at loading rates at or below 0.25 psi/min equilibrium conditions were maintained. During the tests there was no positive visual verification of dewetting, since it was impossible to determine accurately which of the pinholes on the surface had been caused by dewetting and which had been caused by the filler being forced out of the binder during the milling process used to form the specimens.

A digital computer program, utilizing a least squares technique, was written to smooth out the data and plot a curve. The curves were essentially linear above strains of 1.0% and there was an acceptable variation of the Tangent Modulus between tests of less than 10% (Figs. 2 and 3, Table I). The Tangent Modulus obtained from these tests was used in later calculations. The optical tests showed the Modulus of Elasticity of the propellant to be 450 psi in the linear range.

Two tests were made in an attempt to obtain Poisson's Ratio in a similar manner. Poisson's Ratio can be used as a direct indicator of the volume change and thus indicate dewetting. Here the data acquisition method failed completely. The scatter caused by the slippage of the gearing in the comparator alone was sufficient to render the data worthless. The scatter in the data below 1.0% in the stress-strain curves also was too high to be acceptable.

It was then decided to utilize a simple device which had high resolution at low strain levels. Normal strain gages meet this requirement, yet affixing them to the propellant causes an effective stiffening of the propellant in the area of attachment, which restricts the propellant flow in the stiffened area. This situation can be avoided if the cement used to attach the strain gages to the propellant was used to form a sandwich material, which would have uniform properties through its length for any cross-sectional area.

Sandwich Material Theory

This sandwich material was formed by placing a thin, uniform layer of cement on two sides of the propellant in such a manner that the cement would be a load carrying portion of the specimen and have the same total elongation. It was recognized that this would not act as the propellant alone, but a stress analysis could be performed on the material and its mechanical properties determined. Also strain gages could then be attached to the material without appreciably affecting the properties of the material.

The stress analysis proceeded as follows.

Elasticity Solution. If it is assumed that the propellant's upper and lower surfaces are stiffened to the point where its side faces ($x = \pm W$) deform in a parabolic shape when loaded in the Y direction, the requirement then exists that the displacement u is an even function of z, $u(z) = u(-z)$, and an odd function of x, $u(x) = -u(-x)$. (Figure 1 for co-ordinate axis orientation) It can also be assumed that for very low stress ratios ($\sigma_x = R\sigma_y$) the displacement v is a linear function of Y.

The displacements were assumed as follows:

$$u = ax^9 + bx^7z^2 + cx^5z^4 + dx^3z^6 + exz^8$$

$$v = ky$$

$$w = f(x)g(z)$$

where f(x) and g(z) are arbitrary functions of x and z respectively.

These assumed values of the displacements are substituted into the equilibrium and compatibility equations. The arbitrary functions f(x) and g(z) can then be found.

The following boundary conditions must also be satisfied.

a. The net load in the Z direction must vanish at z = t

$$\int_{-W}^{W} \sigma_z \, dx = 0$$

b. The net load in the X direction must equal the applied load in the X direction at x = W.

$$\int_{-t}^{+t} \sigma_x \, dz = 2R\frac{Pt}{A} = 2R\sigma_y t$$

c. The net load in the Y direction must equal the applied load in the Y direction.

$$\int_{-t}^{t} \int_{-w}^{w} \sigma_y \, dx \, dy = 4R\sigma_y t w$$

This results in six equations to be solved simultaneously. It will be noted that there is no mention of matching displacements or stresses at the propellant-cement interface, or of solving for displacements or stresses in the cement layer. It is assumed that if the proper displacement distribution is assumed, the stiffening of the outer surface of the propellant occurs due to a τ_{xz} imposed by the glue. It is also assumed that the cement layer is so thin that there are no changes in displacement in the X and Y direction in the cement.

To completely satisfy the problem then requires that the six equations obtained from the equilibrium equations and the boundary conditions must be satisfied.

This is done by solving the six equations simultaneously. However if the strains ε_x and ε_y are measured at the origin of the coordinate system, the only constant required is e, since at (0,0,t):

$$\varepsilon_x = et^8$$

$$\varepsilon_y = k$$

and both ε_x and ε_y can be measured with the use of strain gages.

Hence to solve for Poisson's Ratio the following procedure is necessary.

Solve the resulting six equations simultaneously, which finally results in:

$$\frac{et^8}{k} = \nu' = \frac{\varepsilon_x}{\varepsilon_y} = -\frac{3}{2} + \left[2\left(\frac{t}{\omega}\right)^2 - \frac{1}{12}\left(\frac{\alpha}{\beta}\right)^2\right] w^8 b + \left[\left(\frac{t}{\omega}\right)^4 - \frac{1}{42}\right] c\omega^8 - \left[\frac{(1-2\nu)(1+\nu)}{(1-\nu)} R\right]$$

where

$$b = \left[\frac{6}{5}\left(\frac{t}{\omega}\right)^2\right] c + \frac{3}{2} \frac{k}{\nu} \frac{\omega^6}{t^2} \left[4\nu^2 + \nu - 1\right]$$

and

$$c = \frac{10}{9}\left\{15 \frac{(1-2\nu)(1+\nu)}{(1-\nu)} Rk - \frac{k}{\omega^8} + \left[5\left(\frac{\alpha}{\beta}\right)^2 \frac{k}{\nu} \frac{\omega^6}{t^2} - 135 \frac{k}{\nu} \omega^4\right]\left[4\nu^2 + \nu - 1\right]\right\}$$

which is an extremely complex equation to solve for ν (a cubic equation with variable coefficients). This solution is good only in the limit case where R is much less that 1.0. There was insufficient equipment to run a test at the stress ratios required.

Approximate Solution. Another solution was obtained by approximating the test specimen with a cylinder of very large radius and relating this solution to the test specimen.

Williams [4] has obtained a solution for an encased hollow cylinder, which can be applied to this problem. The normal interface

pressure is given by:

$$p' = \frac{-\nu\sigma + \nu_c \frac{E}{E_c}\sigma_c}{\frac{b^2}{c^2-a^2}\left(\frac{E}{E_c}\right)\left[(1-\nu_c)+(1+\nu_c)\frac{c^2}{b^2}\right]+\frac{b^2}{b^2-a^2}(1-\nu)}$$

where the subscript c denotes case properties.

For a solid cylinder, a = 0 and

$$p' = \frac{-\nu\sigma + \nu_c \frac{E}{E_c}\sigma_c}{(1-\nu)+\frac{b^2}{c^2}\left(\frac{E}{E_c}\right)\left[(1-\nu_c)+(1+\nu_c)\frac{c^2}{b^2}\right]} \qquad (2.1)$$

and

$$\varepsilon_\theta = \frac{-1}{E_c}\left\{\sigma_c\nu_c - \frac{2b^2p'}{c^2-b^2}\right\} \qquad (2.2)$$

$$\varepsilon_z = \frac{2\nu_c}{E_c}\left\{\sigma_c\nu_c - \frac{b^2p'}{c^2-b^2}(1-\nu_c)\right\} \qquad (2.3)$$

if ε_θ and ε_z are measured on the outer surface.

If the analogy is made between $\varepsilon_\theta / \varepsilon_z$ in the uniaxial case on the cylinder to $\varepsilon_x / \varepsilon_y$ on the rectangular test specimen, and further define $\varepsilon_x / \varepsilon_y$ as the apparent Poisson's Ratio ν', then

$$\nu'\left\{2\nu_c\left[\nu_c\sigma_c - \frac{b^2p'}{c^2-b^2}(1-\nu_c)\right]\right\} = -\left\{\nu_c\sigma_c - \frac{2b^2p'}{c^2-b^2}\right\} \qquad (2.4)$$

solving 2.4 for p'

$$p' = \left[\frac{2\nu_c^2 \sigma_c - \nu_c \sigma_c}{2\nu_c \nu' - 2\nu_c^2 \nu' + 2} \right] \left[2\left(\frac{h}{b}\right) + \left(\frac{h}{b}\right)^2 \right] \qquad (2.5)$$

Substituting 2.1 into 2.5 and using the fact that in a rectangular sandwich specimen for unit width [1] :

$$\sigma = \frac{EP}{Eb + E_c h} \qquad \sigma_c = \frac{E_c P}{Eb + E_c h}$$

Yields

$$\frac{-\nu E + \nu_c E_c}{(1-\nu) + \frac{E}{E_c}\left[\frac{b^2}{b^2 + 2bh + h^2}\right](1-\nu_c) + \frac{E}{E_c}(1+\nu_c)}$$

$$= \left[\frac{2\nu_c^2 E_c - \nu_c E_c}{2\nu_c \nu' - 2\nu_c^2 \nu' + 2} \right] \left[2\left(\frac{h}{b}\right) + \left(\frac{h}{b}\right)^2 \right]$$

clearing the denominator, and specifying that h is much less than b, and solving

$$\nu \cong \left\{ \left[\frac{E_c}{E}\right] \left[\frac{h}{b}\right] \left[\frac{1 - 2\nu_c}{\nu_c \nu' - \nu_c^2 \nu' + 1} + 1 \right] \right\} \nu_c \qquad (2.6)$$

Thus Poisson's Ratio of the propellant can be found using the values of the strain on the external surface.

No attempt was made to obtain the Modulus by use of the sandwich method since the resulting solution is extremely sensitive to the proper measurement of the cement thickness.

Strain Gage Technique. Standard tab end specimens were fabricated from a sheet 4.5 inches square. The finished specimens were 4.5 inches long (exclusive of tabs), 1.0 inch wide, and 0.195 inches thick. A thin layer of SR-4 Strain Gage Cement was applied to both faces and allowed to cure for a minimum of twenty-four hours. After the cement had hardened, BLH type A-7 strain gages were attached to the specimens to measure a Poisson effect.

A small test sample was made of the cement used, and a tensile test was conducted on this specimen to obtain its properties. It was found that the Elastic Modulus was 133,000 psi for the range of strain from 0 to 1000 micro-inches/inch, (Table II, Fig. 4) and Poisson's Ratio to be approximately 0.30.

A tab of the specimen was clamped to a rigid support and the specimen loaded uniaxially. In attempting to reach equilibrium conditions, it was noted that the strain readings had pronounced drift. Since strain gages are normally used on metallic surfaces, they reach thermal equilibrium rapidly; (the metallic surface being a heat sink) so rapidly in fact that switching devices may be used so that only the gage of interest is active, and readings may be taken rapidly with little or no detrimental effects. A propellant, however, is an effective thermal insulator; hence a definite period of time must be allowed for the strain gages to reach thermal equilibrium. In order to preclude any creep effects between readings, no switching device was utilized. Instead each gage was connected to an individual power

source and strain reader. Since the primary concern of the experiment was Poisson's Ratio and relating the differences in initiation and completion of dewetting (i.e., relative results), there was no requirement for absolute calibration of the gages. When setting up a specimen, a minimum of two hours was allowed for the strain circuits to reach thermal equilibrium conditions. This was found to be more than ample time. Loads were applied in increments of 50 grams and the propellant was allowed to reach equilibrium conditions, usually in a matter of a few minutes.

Three tests were conducted. Uniaxial test No. 1 was strained to the point where the cement visibly fractured at approximately 1000 microinches/inch of strain. Uniaxial test No. 2 was strained to 800 microinches/inch of strain and then allowed to stand in an unstressed state for 48 hours. The specimen used in uniaxial test No. 2 was then used again. This was done as a check of the validity of the experiment.

Results

The data obtained were substituted into equation 2.6 and plotted. (Table III, Figs. 5, 6, and 7) In these tests the strain data were accurate to about three microinches/inch of strain due to the experimenter's misuse of the strain reader. A trend check was run on the raw data including this limit on accuracy. It showed the trends indicated by the reduced data were not substantially affected by this error.

It appears that the propellant commences dewetting at approximately 100 microinches/inch of strain and is still in the process of dewetting at 300 microinches/inch. It appears to be complete at about 400 microinches/inch of strain as indicated by the shape of the curves, and in light of subsequent biaxial strain tests.

CHAPTER III

BIAXIAL DEWETTING

Technique

A biaxial test specimen was fabricated by cutting a cross-shaped specimen out of a sheet of propellant 4.5 inches square and 0.195 inches thick. This specimen approximates overlapping two standard tab-ended specimens at 90° angles, (Fig. 1), and is the same type of specimen used by E.R.D.E. [9] in some of their testing. Stop holes were drilled in the propellant at the 90° intersection points in order to relieve any possible stress concentrations. To insure that there was essentially a uniform biaxial strain field in the center of the test specimen, a grid was superimposed on the center of the specimen and then large strains were imposed. The grid deformed uniformly at the center and the deformation appeared proportional to the stress ratio.

A thin layer of SR-4 Strain Gage Cement was applied to both faces and allowed to cure for a minimum of 24 hours. After the cement had hardened, BLH type A-7 strain gages were attached to the specimen to measure Poisson's Ratio. Each gage was connected to an individual power source and reader. Then upon setting up the specimen for testing, a minimum of two hours was allowed for the strain gage circuits to reach equilibrium conditions. Biaxial tests were conducted with two tabs 90° apart clamped to a rigid support and the opposite tabs loaded for a biaxial stress. Loads were then applied so that the smaller

load was increased in steps of 50 grams. Loads were applied and the propellant allowed to reach equilibrium conditions, usually a matter of a few minutes.

Twelve tests were conducted with virgin specimens subjected to stress ratios varying from 2.0 to 5.0. The apparent Poisson's Ratio of the sandwich (ν') was found as follows:

$$\varepsilon_y = \frac{1}{E}\left[\sigma_y - \nu'\sigma_x\right]$$

$$\varepsilon_x = \frac{1}{E}\left[\sigma_x - \nu'\sigma_y\right]$$

but $\sigma_x = R\sigma_y$ hence

$$\frac{\varepsilon_x}{\varepsilon_y} = \frac{R - \nu'}{1 - R\nu'}$$

$$\nu' = \frac{\varepsilon_x/\varepsilon_y - R}{R\,\varepsilon_x/\varepsilon_y - 1} \qquad (3\text{-}1)$$

The values of $\varepsilon_x / \varepsilon_y$ were substituted into equation 3.1 for ν' and this value was substituted into 2.6 for ν of the propellant. The results were plotted as ν vs strain. (Table IV, Figs. 8, 9, 10, 11)

Results

The double thickness of the cement (the sum of the thicknesses of both sides), was measured and found to vary from less than 0.001 to greater than 0.002 inches. It became apparent that those tests

which had the extremely thin layer of cement (less than 0.001 in.; the exact value was indeterminate due to the inaccuracy of the measuring devices available), produced poor results due to early fracture of the cement. Cement double thicknesses greater than 0.002 inches produced too stiff a covering, and this appeared to mask the properties of the propellant. This masking can be explained by a simple analogy. If the propellant had been covered with a layer of high tensile steel of equal thickness to the test specimen, the propellant would have had inconsequential effects on the layer of steel and hence strain readings on the outer surface of the steel would give no clue as to the properties of the inner propellant. Hence a cement layer thickness of 0.0005 inches for this propellant specimen-cement combination appeared to be optimum.

Another critical factor was thought to be fabrication techniques. If the propellant was handled so that visible bending took place, the specimen in turn produced results which were incompatible with the results of other tests.

In all, twelve tests were conducted; of these only four were considered of sufficient reliability to be of value. The strain readings were reduced and the data plotted (Figs. 8, 9, 10, 11) as ν vs ε_y.

The first point that can be deduced from these data is that if Farris' model of a propellant, which has a frequency of dewetting directly proportional to the strain-dilatation curve's first derivative with respect to strain [10], is to hold for this propellant, then

dewetting is complete by 300 microinches/inch of strain in all cases. The data below 50 microinches/inch are not sufficiently reliable to conclude where the onset of dewetting occurs. But it appears that the propellant commences dewetting at virtually 0% strain.

Comparison of Results

Comparison to Uniaxial. The biaxial tests indicate dewetting is complete at approximately 300 microinches/inch of strain in all cases. In the biaxial case it appears that dewetting commences at effectively 0% strain.

It appears that the phenomenon may occur at higher strains in the uniaxial case.

Comparison to other Investigations. The previous conclusions do not at first glance appear to agree with the data supplied by the manufacturer, United Technology Corporation. (Fig. 12). These data were obtained using a gas dilatometer. The curve is decaying from the onset of strain to fracture, and this nonlinearity is attributed to dewetting. However, using the standard definition for Poisson's Ratio in a uniaxial stress field from Elasticity,

$$\nu = - \frac{\frac{\Delta W}{W}}{\frac{\Delta L}{L}}$$

and assuming a square cross section for mathematical simplicity and enforcing incompressibility, (no change in volume), the following holds:

$$(L + \Delta L)(W + \Delta W)^2 = LW$$

$$L + \frac{\Delta L}{L} = \left(1 + \frac{\Delta W}{W}\right)^{-2} \qquad (4.1)$$

$$1 + \frac{\Delta W}{W} = \sqrt{\frac{1}{1 + \frac{\Delta L}{L}}}$$

$$-\frac{\Delta W}{W} = 1 - \sqrt{\frac{1}{1 + \frac{\Delta L}{L}}}$$

$$\nu = -\frac{\frac{\Delta W}{W}}{\frac{\Delta L}{L}} = \frac{L}{\Delta L}\left[1 - \sqrt{\frac{1}{1 + \frac{\Delta L}{L}}}\right] \qquad (4.2)$$

and for the case where $\Delta L/L = 0.20$

$$\nu = \frac{1}{.20}\left[1 - \sqrt{\frac{1}{1.2}}\right]$$

$$\nu = 0.436$$

Even though incompressibility was enforced, ($\nu = 0.50$), the ν calculated is 0.436. The curve of equation 4.2 is plotted on Figure 12 for comparison. Thus the standard definition cannot even be held to be approximate at large strains.

Another difference is contained in the definition of strain. For large deformations, strain is no longer $\Delta L/L$. Lindsey [13] has defined the problem as follows:

From Elasticity, strain is defined by considering the square of an infinitesimal line element, $ds^2 - ds_o^2$; hence

$$\left(1 + \frac{\Delta L}{L}\right)^2 = 1 + 2\varepsilon \tag{4.3}$$

If $\Delta L/L$ is small, $(\Delta L/L)^2$ is much less than $\Delta L/L$ or $\Delta L/L$ is much less than 1.0, then

$$\varepsilon = \Delta L/L$$

but if $\Delta L/L$ is not much less than 1.0 (large strain) equation 4.3 must be used. Let

$$E_1 = \frac{\Delta L}{L} \qquad E_2 = \frac{\Delta W}{W}$$

then the volume of the bar becomes

$$(L + \Delta L)(W + \Delta W)^2 = LW^2\left(1 + \frac{\Delta L}{L}\right)\left(1 + \frac{\Delta W}{W}\right)^2 = V$$

$$\frac{V}{V_o} = (1 + E_1)(1 + E_2)^2$$

Casting this expression in terms of ε_{22} and ε_{11}

$$\frac{V}{V_o} = \left(\sqrt{1 + 2\varepsilon_{11}}\right)(1 + 2\varepsilon_{22})$$

dividing by ε_{11}, defining $\nu = -\varepsilon_{11}/\varepsilon_{22}$ and solving for ν,

$$\nu = \frac{1}{2(1 + 2\varepsilon_{11})\varepsilon_{11}}\left[(1 + 2\varepsilon_{11})^{1/2} - \frac{V}{V_o}\right]$$

For variable compressibility let $V = kV_o$ where k is a function of ε_{11} and find the limit of $\nu(\varepsilon_{11})$ as ε_{11} approaches zero.

$$\nu(0) = \frac{1 - \frac{dk}{d\varepsilon_{11}}}{2}$$

thus

$$\frac{dk}{d\varepsilon_{11}} = 1 - 2\nu(0)$$

Integrating

$$k = [1 - 2\nu(0)]\varepsilon_{11} + C_1$$

For $\nu(0) = 1/2$, $k = 1$ which makes it possible to evaluate C_1

$$k = 1 = [1 - 2\nu(0)]\varepsilon_{11} + 1$$

or

$$C_1 = 1$$

The expression for Poisson's Ratio now becomes,

$$\nu = \frac{1}{2\varepsilon_{11}}\left[1 - \frac{[1 - 2\nu(0)]\varepsilon_{11} + 1}{(1 + 2\varepsilon_{11})^{1/2}}\right] \qquad (4.4)$$

Thus for UTC data (Fig. 12) at the lowest strain rate, (which is close to the equilibrium conditions used), a $\Delta L/L = 0.20$ substituted into equation 4.3 yields $\varepsilon_{11} = 0.22$. Substituting this value into

equation (4.4) yields $\nu(0) = 0.49$, which when compared to the results obtained in the sandwich tests indicates that there is little difference between the results obtained in this experiment and those obtained by UTC.

Thus a major point may be made. The non-linearities of strain-dilatation curves or Poisson's Ratio vs strain curves, (such as UTC's) which are normally attributed to the process of dewetting through the entire strain area, are in reality caused by:

1) The error in defining Poisson's Ratio as $\Delta W/W / \Delta L/L$ for large strain, and

2) the dependence on the value of $\nu(0)$ (Eq. 4.4).

$\nu(0)$ is a slightly lower value than 0.50 due to the dewetting, which is complete at so low a strain (400 microinches/inch) that it is effectively zero. (hence $\nu(0) = 0.49$). Dewetting is then a phenomenon which occurs at very low strain in this propellant and affects the strain dilatation curves by effectively shifting the value of $\nu(0)$.

The conclusion may be drawn that the major criterion for dewetting in a biaxial stress field is still the maximum principal strain, but this value of strain decreases with increasing stress ratio. This conclusion is analagous to the results of Spangler [6] in his tests relating fracture to strain. This also agrees with the results of experimenters who worked with uniaxial stresses, i.e., Smith [2], and Rainbird and Vernon [5].

CONCLUSIONS AND RECOMMENDATIONS

The technique of a sandwich specimen appears to be useful and worthy of further testing and for use in testing of propellant for other properties, e.g., viscoelastic Poisson's Ratio. However, rather than using a material such as cement to stiffen the outer surface of the propellant, some other material such as commercially available aluminum or brass foil, which is available with thicknesses of the order of 0.00015 inches, should be considered. This foil would have a constant and controllable thickness, and hence lend itself to more reproducible data. It appears that the parameter $E_c/E \cdot h/b$ is a good criterion for the effectiveness of the covering material.

The onset of dewetting occurs at so low a strain in this propellant that it can be considered to start at zero strain, and is complete at so low a strain that the phenomenon can be excluded from any practical engineering considerations.

Dewetting is completed at lower strain values for higher stress ratios. The major criterion is the maximum principal strain.

The normal definition of Poisson's Ratio is invalid for large strain, and care should be exercised in the use of this relationship in analytic or experimental work.

BIBLIOGRAPHY

1. Roark, R. J. Formulas for Stress and Strain, 3rd ed. New York: McGraw Hill Book Co., 1954: 79

2. Smith, T. S. Volume changes and dewetting in glass bead-polyvinyl chloride elastomeric composites under large deformations. Transactions of the Society of Rheology. v. 3, 1959.

3. Stedry, P. J., Landel, R.F., Shelton, H.T. Volume changes and Poisson's Ratio of polyurethane propellants under tensile deformations. Jet Propulsion Laboratory, California Institute of Technology Technical Report No. 32-168, 1961.

4. Williams, M. L., Blatz, P.J., Schapery, R.A. Fundamental studies relating to systems analysis of solid propellants. Final Report-Graduate Aeronautical Laboratories, California Institute of Technology, GALCIT-101. Feb 1961. pp 149-150

5. Rainbird, R. W., Vernon, J.H.C., Solid propellants: studies on dewetting due to strain. Explosives Research and Development Establishment Technical Memorandum No. 7/M/61, Sept 1961

6. Spangler, R.D. A biaxial stress-strain test for solid rocket propellants. E. I. du Pont de Nemours and Co., Gillistown, New Jersey. Presented at the 20th Meeting Joint Army-Navy Air Force-ARPA-NASA Panel on Physical Properties of Solid Propellants, Riverside, California. Nov. 1961

7. Rastrelli, L.V., Dehart, R.C. Measurements of strains in solid propellant grains. Southwest Research Institute. Presented at the 20th Meeting, Joint Army-Navy-Air Force-ARPA-NASA Panel on Physical Properties of Solid Propellants, Riverside, California. Nov. 1961.

8. Bells, K.W., Jr., Hart, W. D., Holland, W. E., Effect on dewetting and volume changes on the tensile behavior of solid composite propellants. Aerojet General Corporation, Azusa. Presented at the 20th Meeting, Joint Army-Navy-Air Force-ARPA-NASA Panel on Physical Properties of Solid Propellants, Riverside, California Nov.1961

9. Rainbird, R.W., Vernon, J.H.C. The Behavior of solid propellants under biaxial tensile stresses. Explosives Research and Development Establishment Report No. 3/R/64, April 1964

10. Farris, R.J. Strain dilitation in solid propellants. Bulletin of 3rd Annual Meeting of ICRPG Solid Propellant Working Group on Mechanical Behavior. CPIA Publication No. 61U, v. 1. October 1964. p 291

11. Farris, R.J. The influence of vacuole formation on the response and failure of solid propellants. Bulletin of 4th Annual Meeting of ICRPG Solid Propellant Working Group on Mechanical Behavior, CPIA Publication No. 94U, October 1965

12. Thiokol Chemical Corporation. Investigation of broad spectrum volumetric response in solid propellants. Air Force Technical Report AFRPL-TR-65-113. June 1965

13. Lindsey, G.H. Elastic Poisson's Ratio. Unpublished notes, Naval Postgraduate School, Monterey, California May 1967

TABLE I

(A)

STRESS STRAIN IN PROPELLANT

OPTICAL DERIVATION

STRESS RATE = 0.25 psi/min

LOAD (lb)	STRESS (psi)	STRAIN (%)	LOAD (lbs)	STRESS (psi)	STRAIN (%)
0.1	1.26	0.31	0.2	2.52	0.84
0.3	3.79	1.25	0.4	5.05	1.71
0.5	6.31	2.22	0.6	7.57	2.44
0.7	8.84	2.57	0.8	10.10	3.18
0.9	11.36	3.45	1.0	12.62	3.57
1.1	13.89	3.40	1.2	15.15	4.09
1.3	16.41	4.36	1.4	17.67	4.51
1.5	18.93	4.83	1.6	20.20	5.71
1.7	21.46	5.51	1.8	22.72	5.91
1.9	23.98	5.92	2.0	25.28	6.41
2.5	31.56	7.73	3.0	37.87	8.80
3.5	44.18	9.90	4.0	50.49	11.44
4.5	56.80	12.67	5.0	63.17	14.36
5.5	69.42	15.89	6.0	75.74	18.35

TABLE I

(B)

STRESS STRAIN IN PROPELLANT

OPTICAL OBSERVATION

STRESS RATE = 0.11 psi/min

LOAD (lb)	STRESS (psi)	STRAIN (%)	LOAD (lb)	STRESS (psi)	STRAIN (%)
0.2	1.07	0.47	0.4	2.14	0.73
0.6	3.21	1.48	0.8	4.27	1.41
1.0	5.34	1.39	1.2	6.41	1.78
1.4	7.48	1.77	1.6	8.55	1.72
1.8	9.62	2.48	2.0	10.68	2.70
2.2	11.75	3.30	2.4	12.82	3.40
2.6	13.89	3.42	2.8	14.96	3.64
3.0	16.03	3.60	3.2	17.09	3.78
3.4	18.16	4.09	3.6	19.23	4.27
3.8	20.30	4.46	4.0	21.37	4.58
4.2	22.44	5.08	4.4	23.50	5.33
4.6	24.57	5.55	4.8	25.64	5.86
5.0	26.71	5.93	5.2	27.78	6.37
5.4	28.85	6.46	5.6	29.91	6.37
5.8	30.98	7.71			

TABLE II

STRESS STRAIN IN ADHESIVE

LOAD (gram)	STRESS (psi)	STRAIN (μin/in)
50	13.7	150
100	27.1	270
150	40.7	365
200	54.3	450
250	67.8	545
300	81.4	630
350	95.0	735
400	108.5	810
450	122.1	920
500	135.7	995
550	149.3	1075
600	162.8	1170
650	176.4	1215
700	190.0	1285
750	203.5	1410
800	217.1	1480
850	230.7	1550
900	244.2	1620
950	257.8	1685
1000	271.4	1745
1050	284.9	1815
1100	298.5	1865
1150	312.1	1945

TABLE III

(A)

STRESS STRAIN IN PROPELLANT

STRAIN GAGE DATA

UNIAXIAL 1

LOAD (gram)	ε_y (μin/in)	ε_x (μin/in)	ν'	ν
50	14	-7	.500	.4980
100	27	-14	.519	.4985
150	41	-21	.512	.4985
200	52	-26	.500	.4980
250	64	-34	.531	.4990
300	82	-44	.536	.4995
350	97	-51	.528	.4990
400	112	-55	.491	.4975
450	130	-63	.484	.4970
500	147	-69	.469	.4965
550	162	-74	.457	.4960
600	182	-82	.451	.4955
650	201	-87	.433	.4945
700	222	-94	.423	.4940
750	242	-102	.421	.4940
800	271	-105	.387	.4925
850	282	-112	.397	.4930
900	302	-116	.384	.4925

TABLE III

(B)

STRESS STRAIN DATA IN PROPELLANT

STRAIN GAGE DATA

UNIAXIAL 2

LOAD (gram)	ε_y (μin/in)	ε_x (μin/in)	ν'	ν
50	0	-1	-	-
100	5	-2	.400	.4930
150	17	-12	.705	.5080
200	34	-17	.500	.4985
250	47	-26	.553	.500
300	64	-31	.484	.4970
350	77	-40	.519	.4985
400	97	-41	.422	.4940
450	114	-52	.456	.4955
500	130	-58	.446	.4955
550	146	-64	.438	.4950
600	167	-71	.425	.4945
650	186	-76	.409	.4935
700	205	-86	.420	.4940
750	226	-88	.389	.4925
800	247	-93	.377	.4920
850	268	-96	.358	.4915
900	293	-101	.345	.4910
950	316	-104	.329	.4900
1000	340	-113	.333	.4905
1050	360	-129	.358	.4915

TABLE III

(C)

STRESS STRAIN DATA IN PROPELLANT

STRAIN GAGE DATA

UNIAXIAL 2 RERUN

LOAD (gram)	ε_y (μin/in)	ε_x (μin/in)	ν'	ν
100	77	-22	.285	.4885
200	149	-45	.302	.4890
300	226	-68	.301	.4890
400	302	-90	.300	.4890
500	382	-115	.301	.4890
600	460	-138	.300	.4890
700	543	-160	.295	.4885
800	620	-181	.290	.4885
900	692	-204	.295	.4885
1000	845	-226	.294	.4885

TABLE IV

(A)

STRESS STRAIN DATA IN PROPELLANT

STRAIN GAGE DATA

BIAXIAL 1 ($\varepsilon_y / \varepsilon_x = 2.0$)

LOAD (gram)	ε_y (in/in)	ε_x (in/in)		
100	90	18	.333	.4905
200	164	31	.343	.4905
300	216	50	.304	.4890
400	314	71	.310	.4895
500	400	91	.308	.4890
600	480	112	.302	.4890
700	564	128	.308	.4890
800	652	150	.305	.4890

TABLE IV

(B)

STRESS STRAIN DATA IN PROPELLANT

STRAIN GAGE DATA

BIAXIAL 2 ($\sigma_y / \sigma_x = 2.0$)

LOAD (gram)	ε_y (μin/in)	ε_x (μin/in)	ν'	ν
100	18	-9	.800	.5125
200	40	-5	.589	.5020
300	70	0	.500	.4980
400	95	21	.451	.4955
500	125	26	.431	.4945
600	165	26	.449	.4955
700	200	34	.434	.4945
800	232	40	.414	.4940
900	271	45	.412	.4940
1000	310	54	.399	.4930
1100	349	63	.391	.4930
1200	383	85	.372	.4920
1300	422	94	.366	.4915
1400	462	103	.366	.4915
1500	503	110	.362	.4915

TABLE IV

(D)

STRESS STRAIN DATA IN PROPELLANT

STRAIN GAGE DATA

BIAXIAL 4 ($\sigma_y / \sigma_x = 3.0$)

LOAD (gram)	ε_y (μin/in)	ε_x (μin/in)	ν'	ν
150	161	34	.508	.4980
300	288	45	.465	.4960
450	414	66	.467	.4960
600	543	93	.477	.4965
750	682	125	.486	.4970
900	816	134	.471	.4965
1050	950	148	.465	.4960

TABLE IV

(E)

STRESS STRAIN DATA IN PROPELLANT

STRAIN GAGE DATA

BIAXIAL 5 ($\sigma_y / \sigma_x = 5.0$)

LOAD (gram)	ε_y (μin/in)	ε_x (μin/in)	ν'	ν
250	60	-15	.434	.4950
500	140	-25	.366	.4915
750	230	-35	.329	.4900
1000	335	-45	.325	.4900
1250	430	-55	.308	.4890
1500	520	-65	.317	.4895

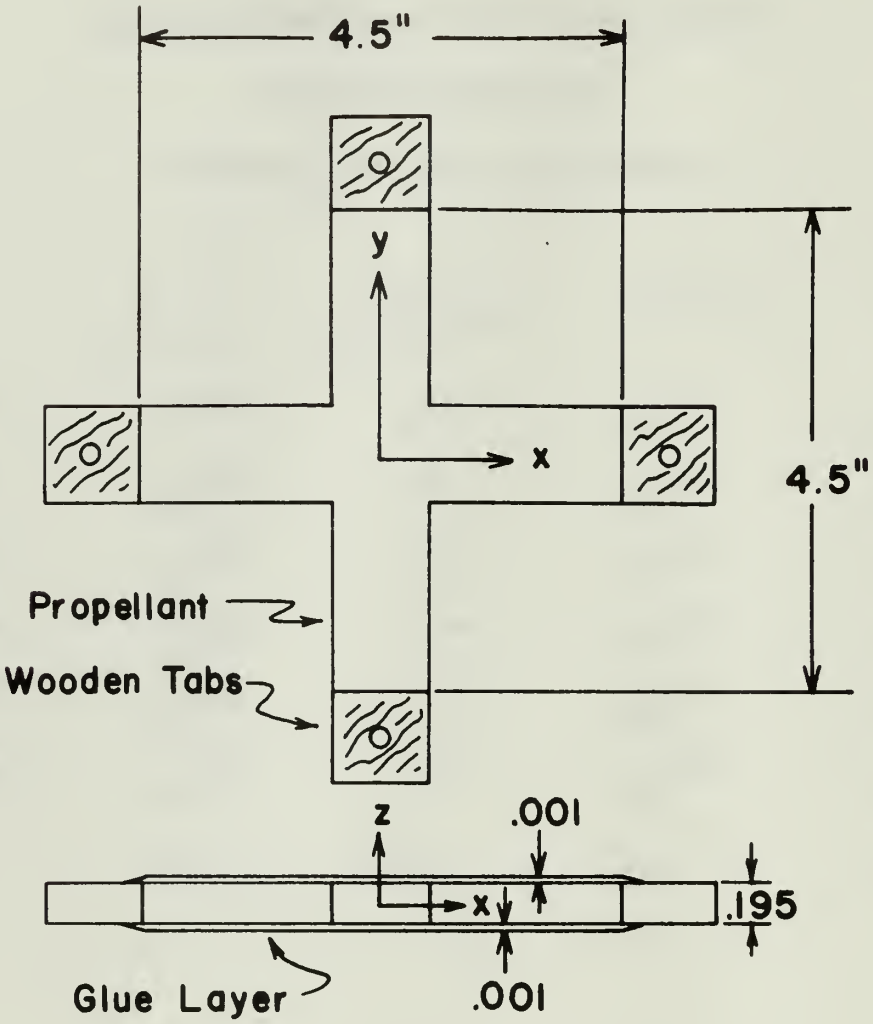

FIGURE 1

PROPELLANT TEST SPECIMEN
(INCLUDING CO-ORDINATE AXIS)

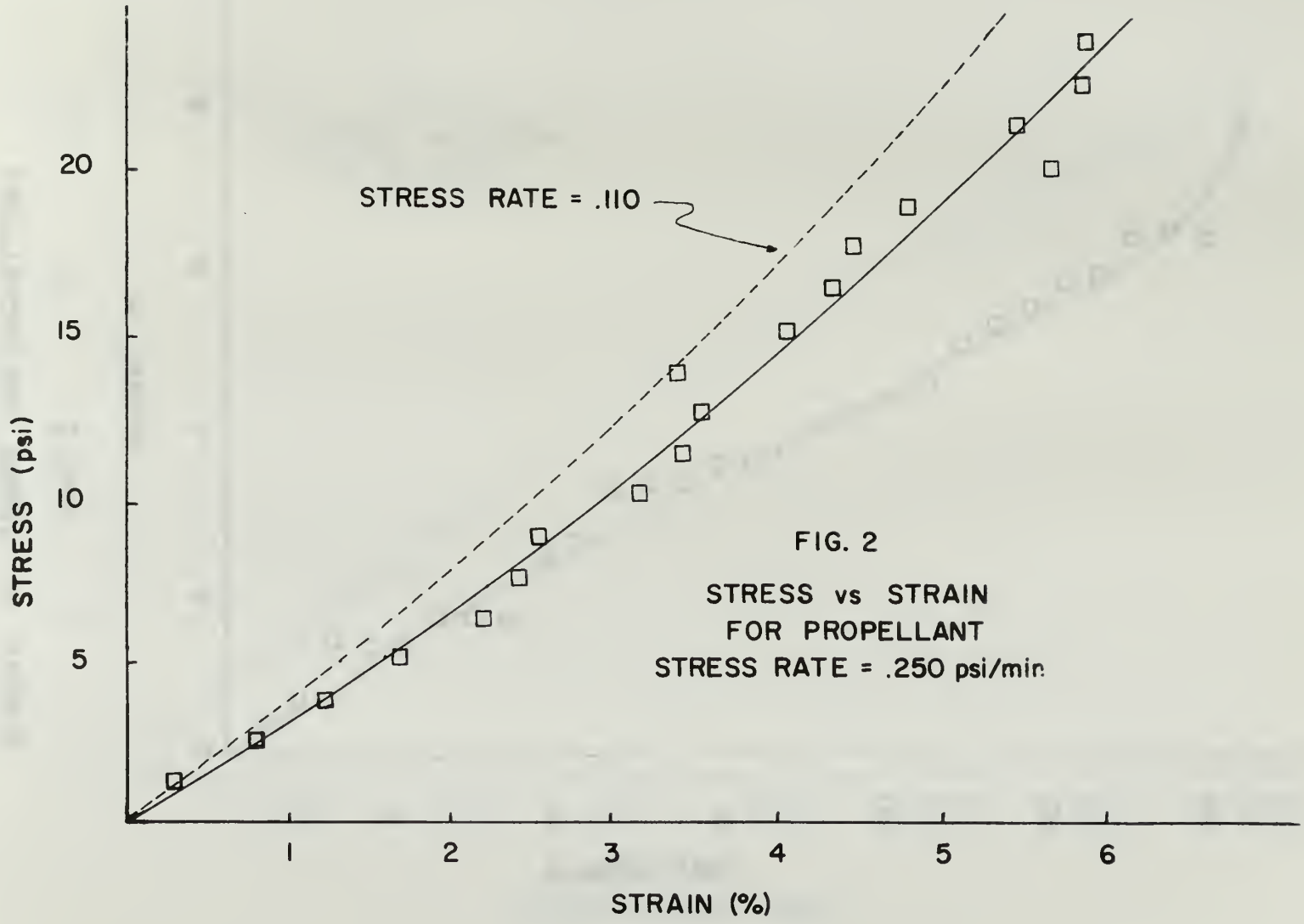

FIG. 2

STRESS vs STRAIN
FOR PROPELLANT
STRESS RATE = .250 psi/min

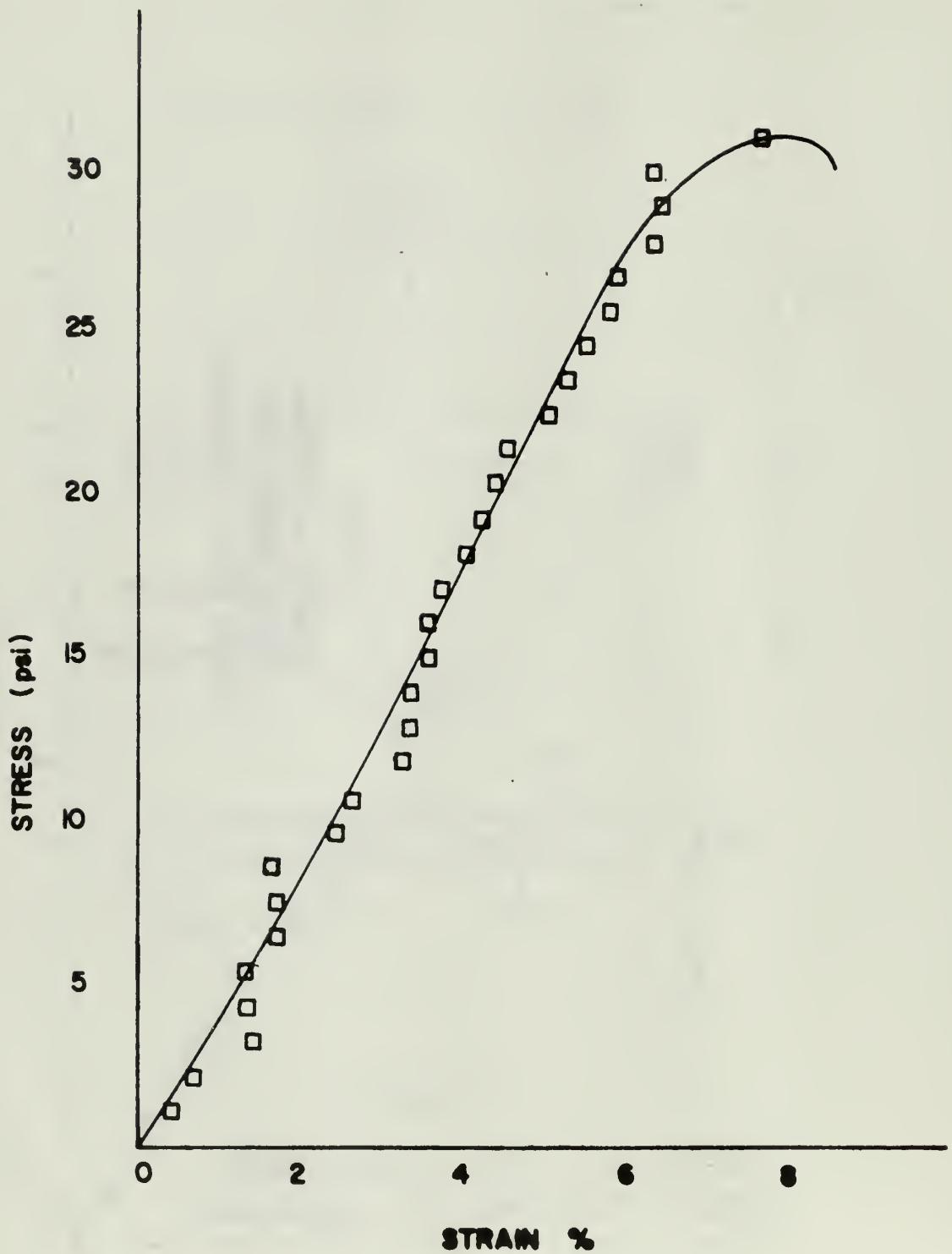

FIG. 3

STRESS vs STRAIN FOR PROPELLANT

STRESS RATE = .110 psi/min

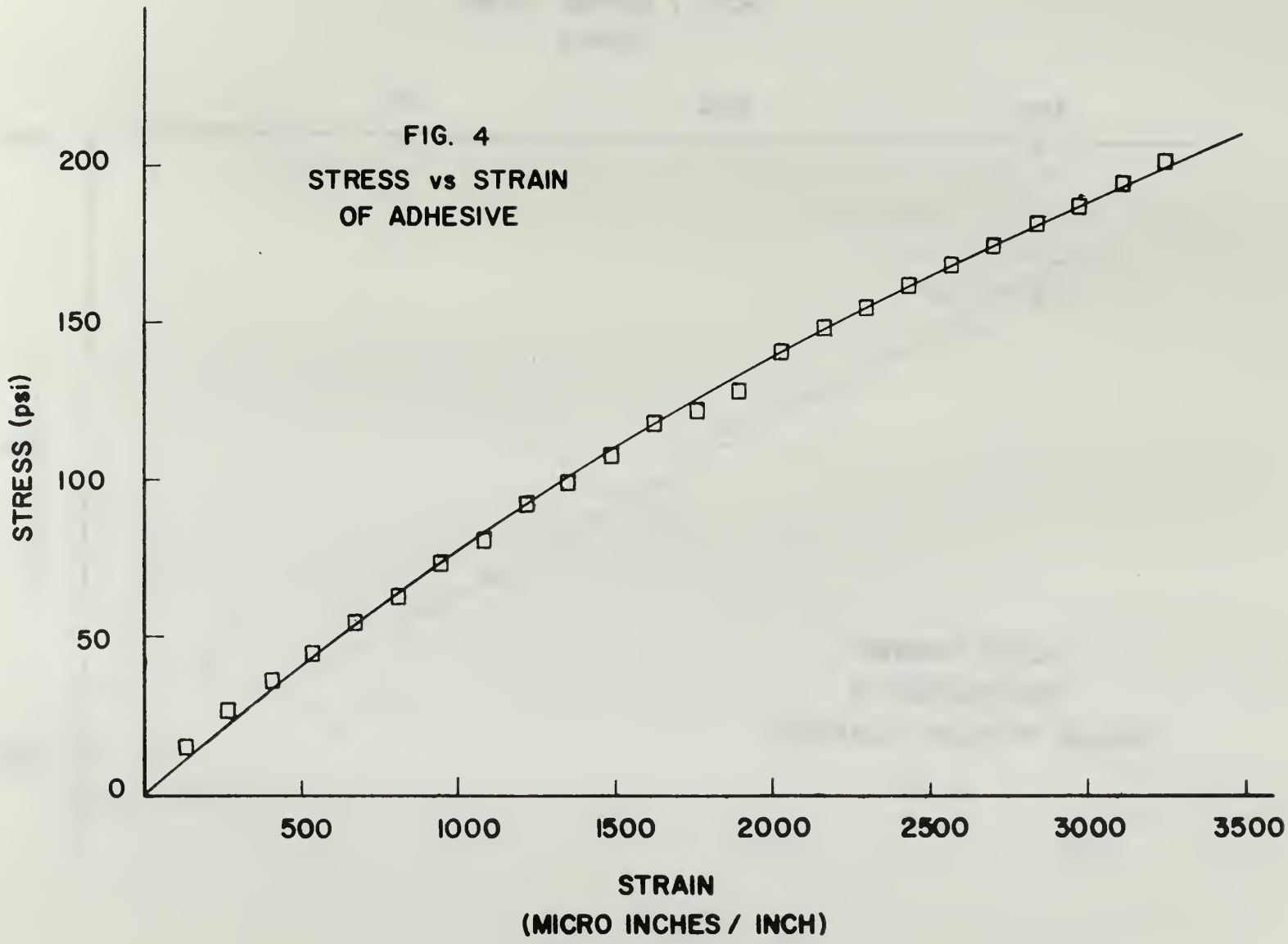
FIG. 4
STRESS vs STRAIN
OF ADHESIVE
STRESS (psi)
0
50
100
150
200
500
1000
1500
2000
2500
3000
3500
STRAIN
(MICRO INCHES / INCH)

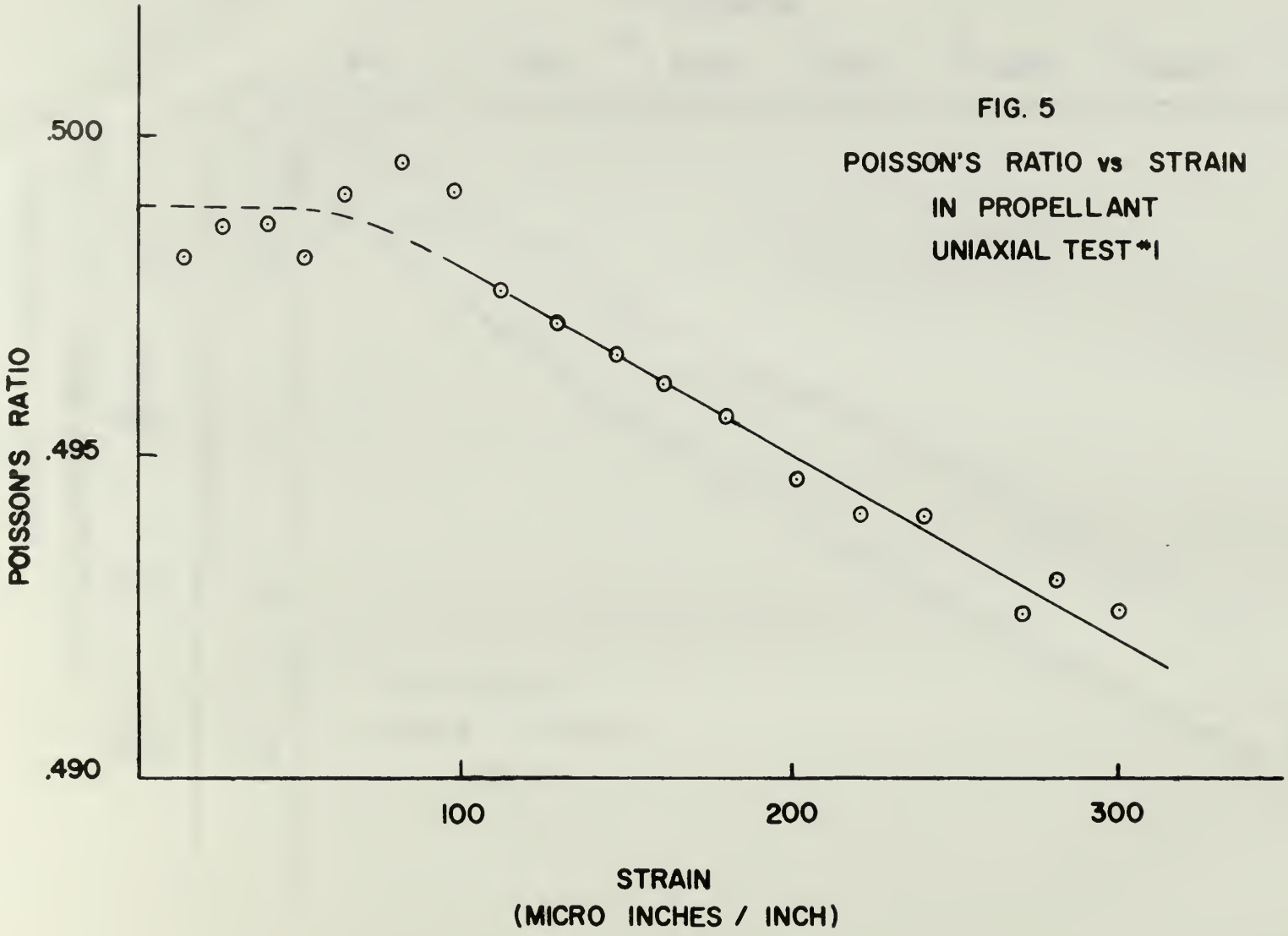

FIG. 5

POISSON'S RATIO vs STRAIN
IN PROPELLANT
UNIAXIAL TEST #1

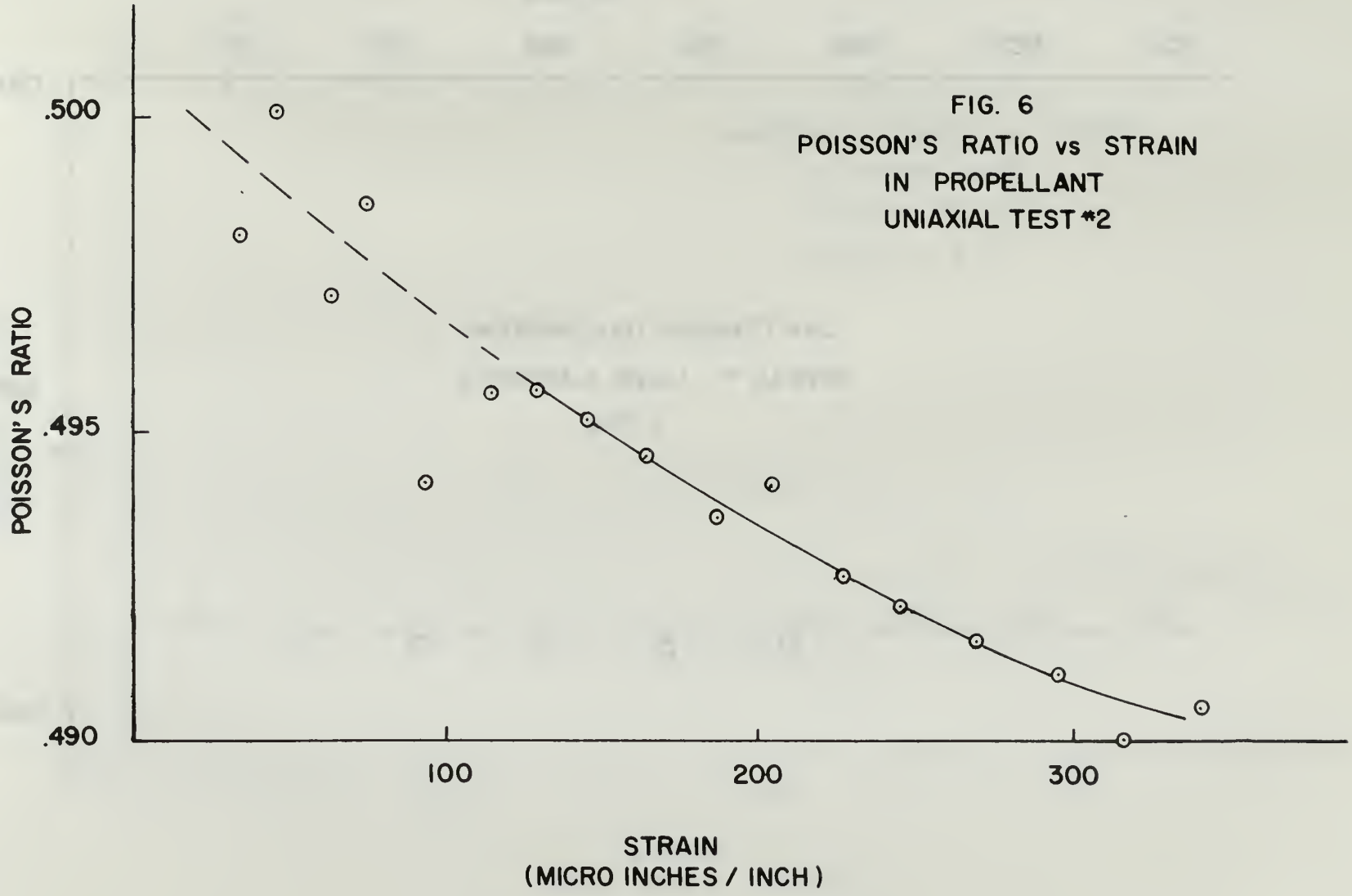

FIG. 6
POISSON'S RATIO vs STRAIN
IN PROPELLANT
UNIAXIAL TEST #2

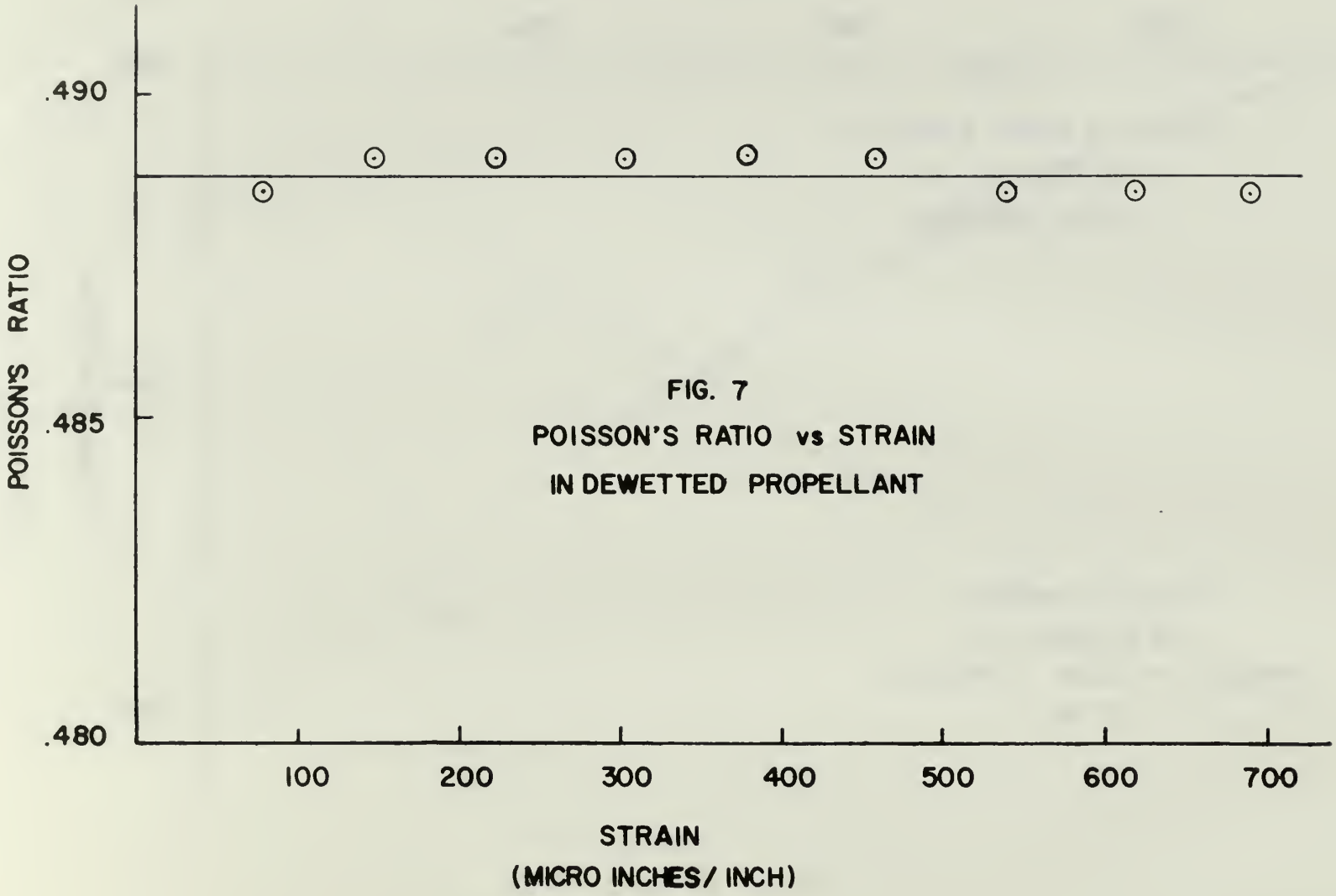

FIG. 7
POISSON'S RATIO vs STRAIN
IN DEWETTED PROPELLANT

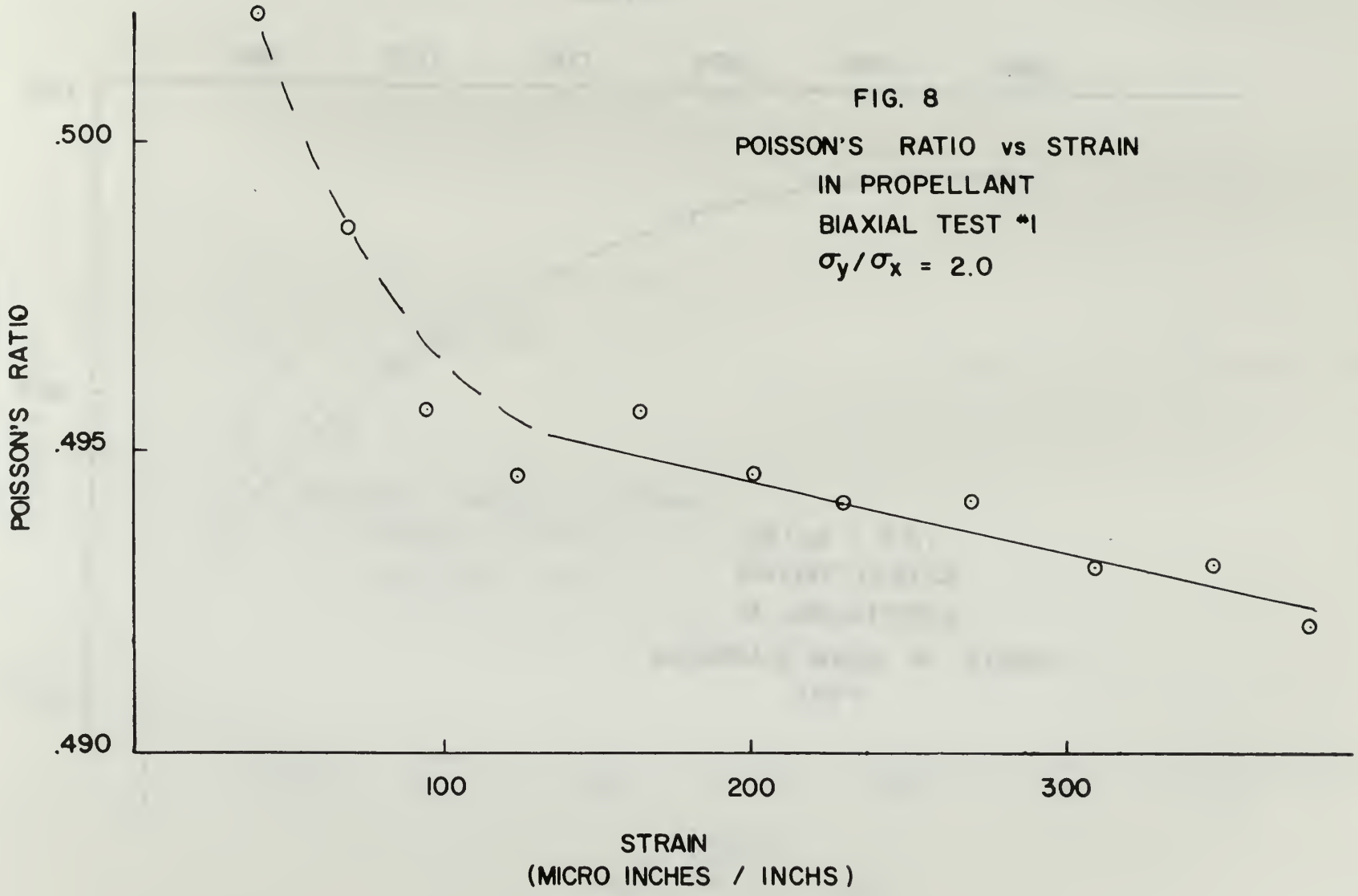

FIG. 8

POISSON'S RATIO vs STRAIN
IN PROPELLANT
BIAXIAL TEST #1
$\sigma_y / \sigma_x = 2.0$

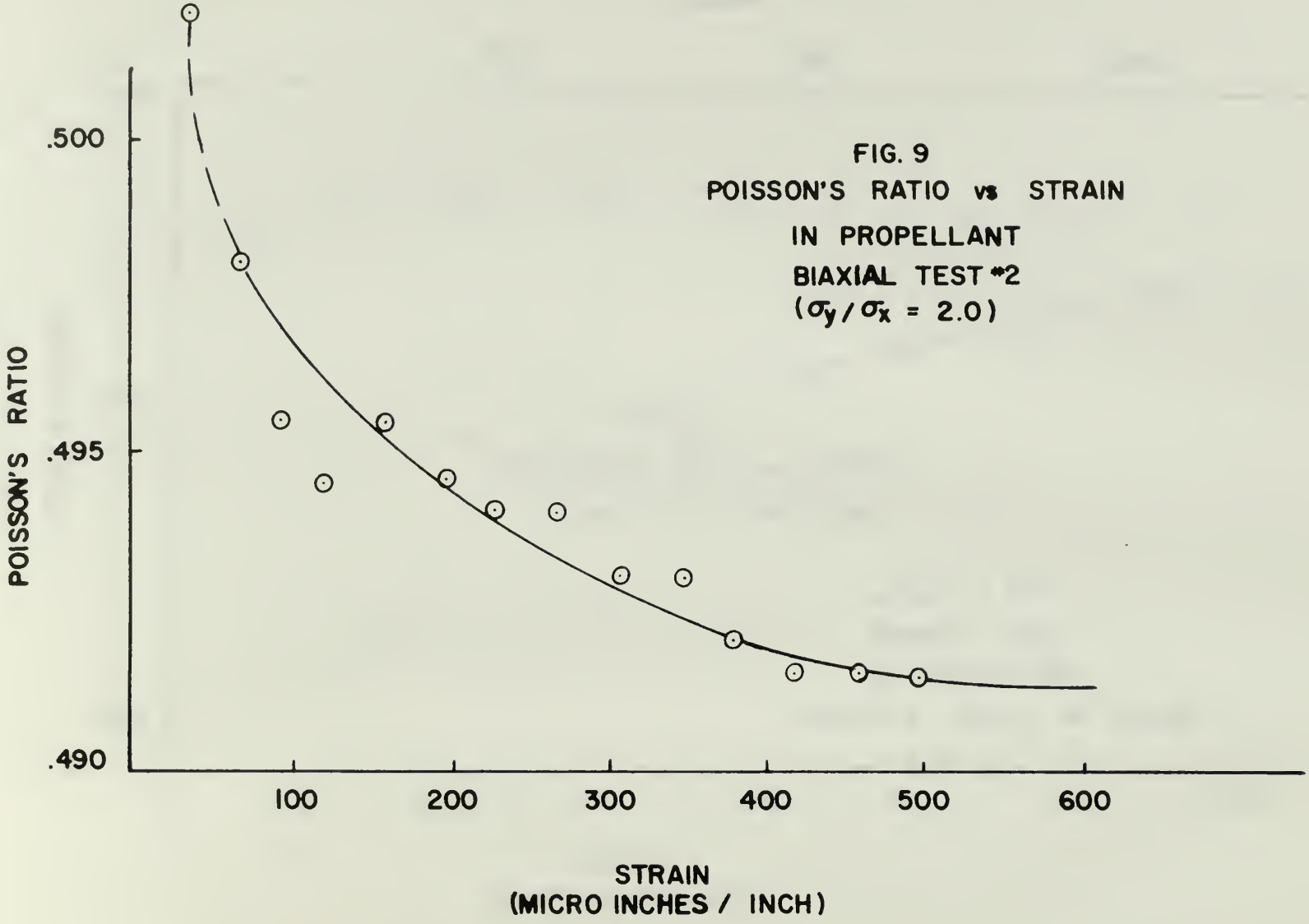

FIG. 9
POISSON'S RATIO vs STRAIN
IN PROPELLANT
BIAXIAL TEST #2
($\sigma_y / \sigma_x = 2.0$)

FIGURE 10

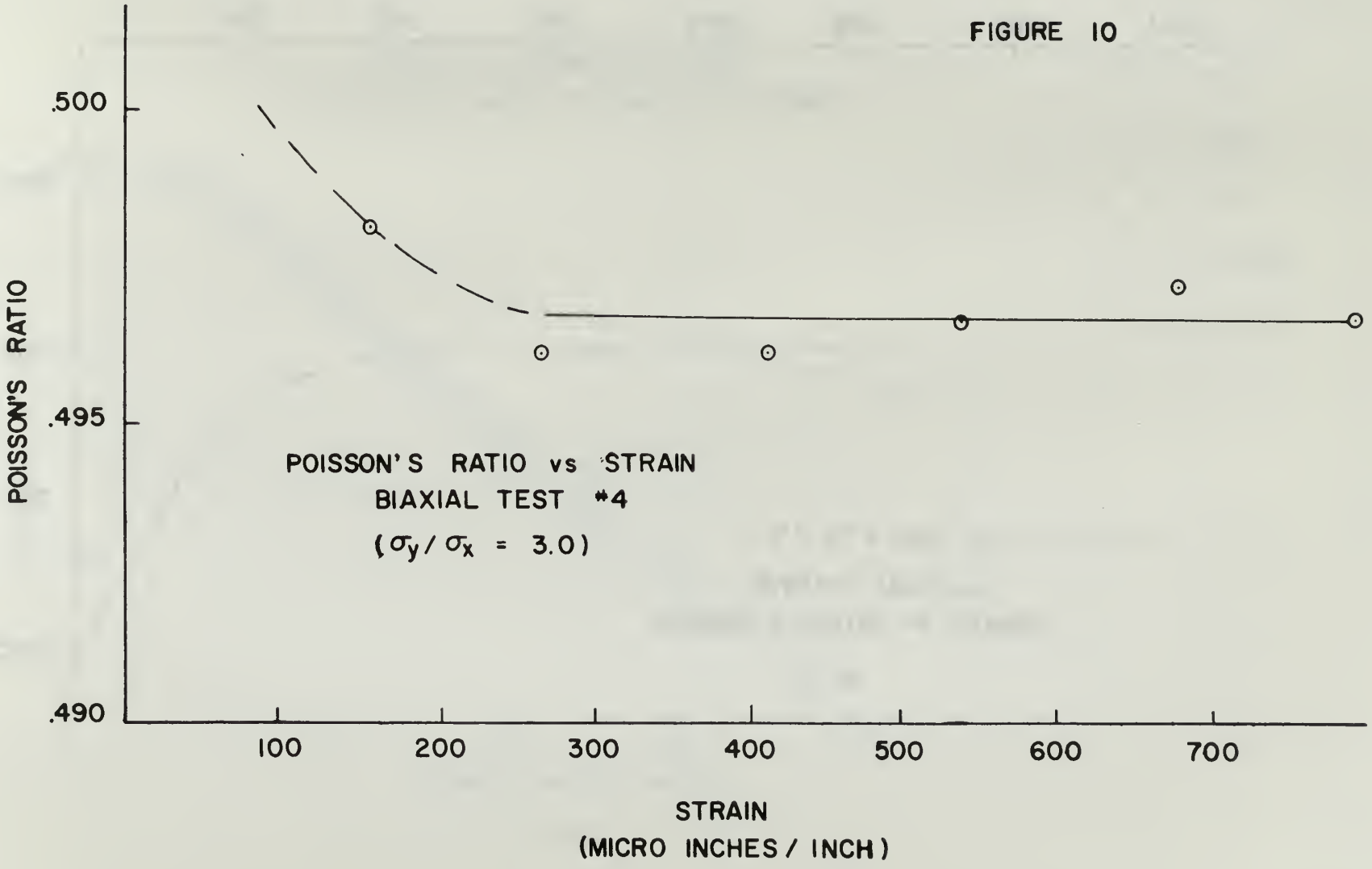
.500
.495
.490
POISSON'S RATIO
100
200
300
400
500
600
700
STRAIN
(MICRO INCHES / INCH)
POISSON'S RATIO vs STRAIN
BIAXIAL TEST #4
(σ_y / σ_x = 3.0)

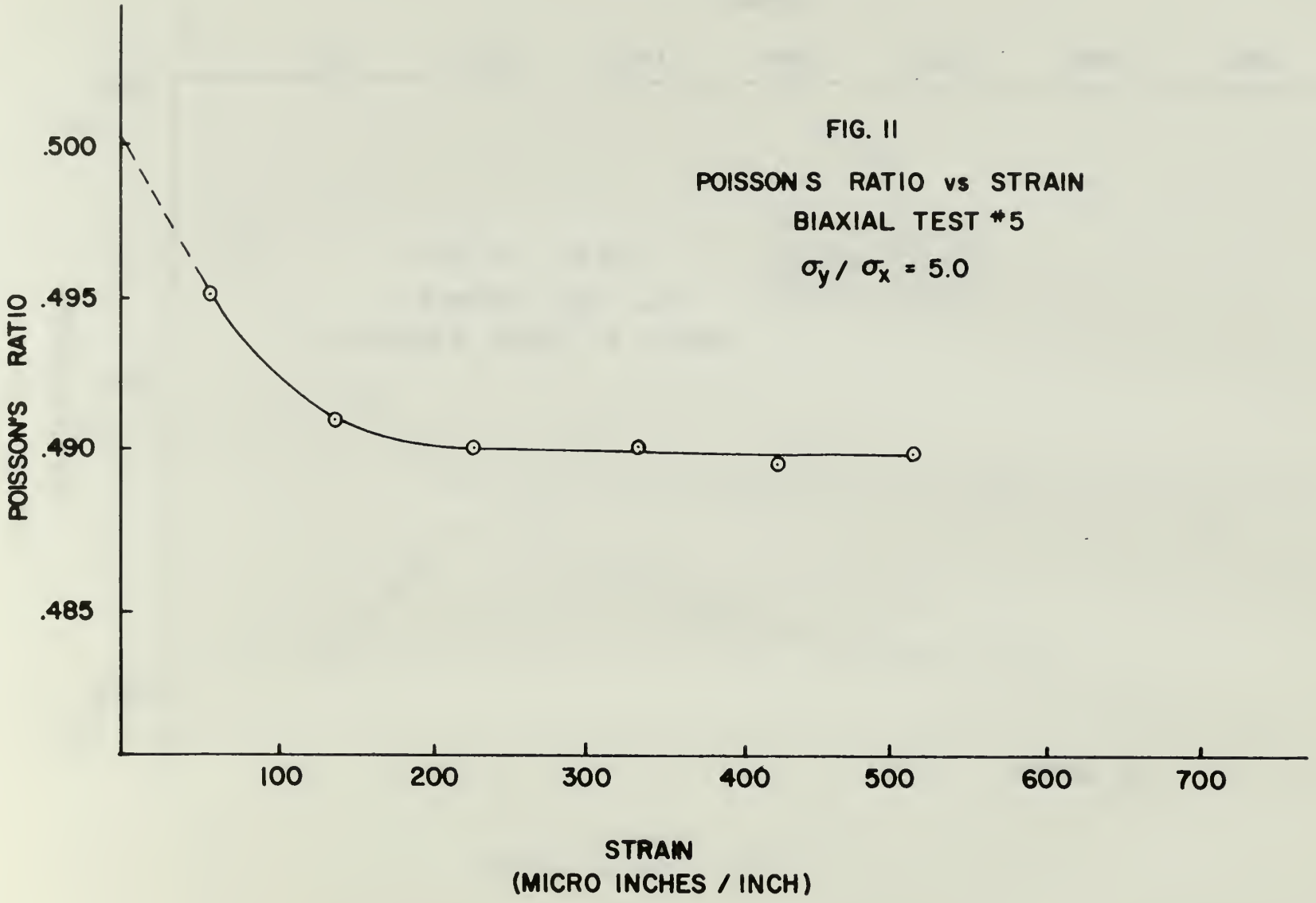
FIG. 11
POISSON S RATIO vs STRAIN
BIAXIAL TEST #5
$\sigma_y / \sigma_x = 5.0$
POISSON'S RATIO
.500
.495
.490
.485
100
200
300
400
500
600
700
STRAIN
(MICRO INCHES / INCH)

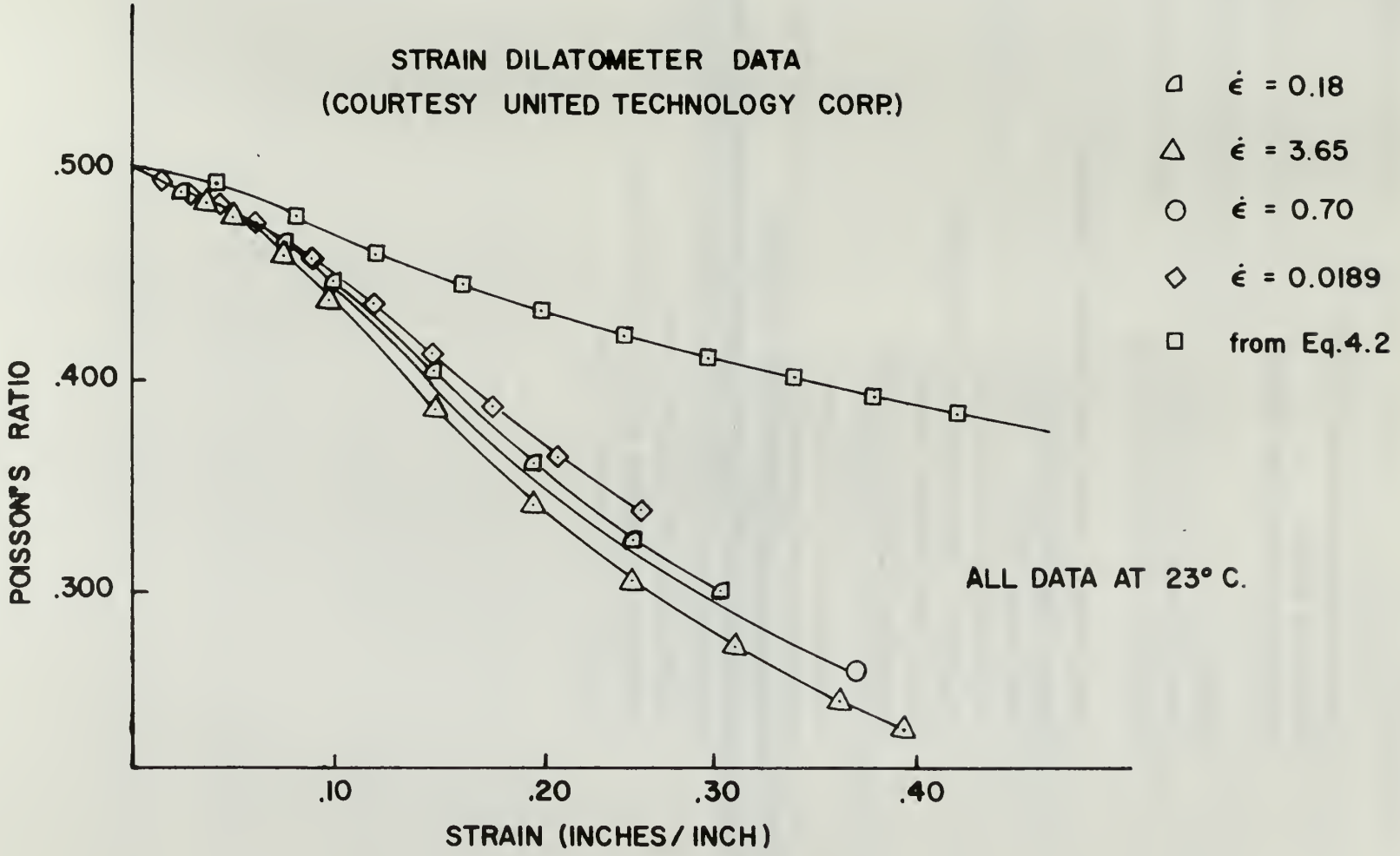
STRAIN DILATOMETER DATA
(COURTESY UNITED TECHNOLOGY CORP.)
$\dot{\epsilon}$ = 0.18
$\dot{\epsilon}$ = 3.65
$\dot{\epsilon}$ = 0.70
$\dot{\epsilon}$ = 0.0189
from Eq.4.2
ALL DATA AT 23° C.
POISSON'S RATIO
.500
.400
.300
.10
.20
.30
.40
STRAIN (INCHES/INCH)

FIG. 12

INITIAL DISTRIBUTION LIST

		No. Copies
1.	Defense Documentation Center Cameron Station Alexandria, Virginia 22314	20
2.	Library Naval Postgraduate School Monterey, California 93940	2
3.	Commander, Naval Air Systems Command Department of the Navy Washington, D. C. 20360	1
4.	Chairman, Department of Aeronautics Naval Postgraduate School Monterey, California 93940	2
5.	Professor G. H. Lindsey Department of Aeronautics Naval Postgraduate School Monterey, California 93940	6
6.	LCDR Julius R. Juliano, USN ATKRON ONE TWO FIVE (VA-125), NAS Lemoore, California 93246	1

DOCUMENT CONTROL DATA - R&D

(Security classification of title, body of abstract and indexing annotation must be entered when the overall report is classified)

1. ORIGINATING ACTIVITY *(Corporate author)*: Naval Postgraduate School, Monterey, California

2a. REPORT SECURITY CLASSIFICATION: Unclassified

2b. GROUP:

3. REPORT TITLE: A Determination of Dewetting in a Biaxial Stress Field

4. DESCRIPTIVE NOTES *(Type of report and inclusive dates)*:

5. AUTHOR(S) *(Last name, first name, initial)*: JULIANO, Julius R.

6. REPORT DATE	7a. TOTAL NO. OF PAGES	7b. NO. OF REFS
June 1967	62	12

8a. CONTRACT OR GRANT NO.:

b. PROJECT NO.:

c.:

d.:

9a. ORIGINATOR'S REPORT NUMBER(S):

9b. OTHER REPORT NO(S) *(Any other numbers that may be assigned this report)*:

10. AVAILABILITY/LIMITATION NOTICES: [redacted]

11. SUPPLEMENTARY NOTES:

12. SPONSORING MILITARY ACTIVITY: Naval Postgraduate School

13. ABSTRACT

An experimental investigation of dewetting in uniaxial and biaxial stress fields was conducted for infinitesimal strain levels. An optical technique was attempted with limited success, which demonstrated the need for more precise measurements at small strains. A method was developed for stiffening the surface of the propellant test specimen with commercial bonding cement, which facilitated the use of strain gages on the stiffened surface. An analytic expression was derived which relates measurements made on the outer surface of the cement to internal propellant behavior.

It was noted that dewetting commenced at strain levels of the order of zero strain, and that there was little variation with stress ratio in the strain at which dewetting commenced. Dewetting appeared to be complete at lower strains for higher stress ratios.

Dewetting was noted to be at such low strain values that the phenomenon is considered to be inconsequential in a practical engineering analysis of this propellant.

DD FORM 1 JAN 64 1473

14. KEY WORDS	LINK A		LINK B		LINK C	
	ROLE	WT	ROLE	WT	ROLE	WT
Propellent						
Dewetting						
Mechanical Properties						